Molecular Biology of the Cell
Vol. 19, 5327–5337, December 2008

SNARE Function Is Not Involved in Early Endosome Docking

Ulf Geumann,* Sina Victoria Barysch,* Peer Hoopmann,*† Reinhard Jahn,* and Silvio O. Rizzoli*†

*Department of Neurobiology, Max Planck Institute for Biophysical Chemistry, Göttingen 37077, Germany; and †European Neuroscience Institute, Göttingen 37077, Germany

Submitted May 6, 2008; Revised August 26, 2008; Accepted September 26, 2008
Monitoring Editor: Jean E. Gruenberg

Docking and fusion of transport vesicles constitute elementary steps in intracellular membrane traffic. While docking is thought to be initiated by Rab-effector complexes, fusion is mediated by SNARE (*N*-ethylmaleimide-sensitive factor [NSF] attachment receptor) proteins. However, it has been recently debated whether SNAREs also play a role in the establishment or maintenance of a stably docked state. To address this question, we have investigated the SNARE dependence of docking and fusion of early endosomes, one of the central sorting compartments in the endocytic pathway. A new, fluorescence-based in vitro assay was developed, which allowed us to investigate fusion and docking in parallel. Similar to homotypic fusion, docking of early endosomes is dependent on the presence of ATP and requires physiological temperatures. Unlike fusion, docking is insensitive to the perturbation of SNARE function by means of soluble SNARE motifs, SNARE-specific F_{ab} fragments, or by a block of NSF activity. In contrast, as expected, docking is strongly reduced by interfering with the synthesis of phosphatidyl inositol (PI)-3 phosphate, with the function of Rab-GTPases, as well as with early endosomal autoantigen 1 (EEA1), an essential tethering factor. We conclude that docking of early endosomes is independent of SNARE function.

INTRODUCTION

The function of the secretory pathway requires transport of material between different intracellular compartments or organelles. This is achieved by organelle budding and fusion, two processes that are highly controlled within the cell. In order for two organelles to fuse, they need to first undergo docking and then priming, an ATP-dependent process that sets up the fusion machinery (Kawasaki *et al.,* 1998; Klenchin and Martin, 2000).

Docking, defined as the close contact of two membranes in preparation of fusion (Schikorski and Stevens, 2001), is thought to be controlled by Rab/Ypt GTPases and initialized by specialized tethering molecules bridging the organelles (Sztul and Lupashin, 2006). Several such tethers (generally large coiled-coil proteins or multisubunit complexes) are known (Waters and Hughson, 2000). Tethers may be directly recruited by activated GTPases, as for example the GARP (Golgi-associated retrograde protein) complex in retrograde trafficking. Alternatively, they may contain a guanine nucleotide exchange factor (GEF) activity such as the transport protein particle (TRAPP 1) complex, which activates the GTPase Ypt1p and functions in ER-to-Golgi traffic. Both activities may also be combined, such as in the vacuolar HOPS (homotypic fusion and vacuole protein sorting) complex, which does not only act as a GEF but also as an effector for Ypt7p. Some of these tethers like the HOPS and Dsl1 complex have also been implicated in SNARE (*N*-ethylmaleimide-sensitive factor [NSF] attachment receptor) binding, which would provide a link to the core fusion machinery (for review see Cai *et al.,* 2007).

SNARE proteins deliver the energy necessary for membrane fusion through the interaction of SNAREs from two opposing membranes and formation of a four-helical bundle: the *trans*-complex. Complex formation is initiated at the N-terminus of the SNARE motif, which is found distal from the membrane, and proceeds toward the membrane-proximal C-terminus (in a process termed "zippering"), thereby pulling the membranes together and overcoming the energy barrier. After fusion, all SNAREs of the complex are located in the same membrane, in what is termed *cis*-complexes. These are nonproductive in terms of fusion and need to be disassembled to provide free SNARE molecules for future rounds of fusion, a process achieved by the AAA-ATPase NSF and its cofactor αSNAP (soluble NSF attachment protein), in an energy-dependent process (Jahn and Scheller, 2006).

One of the trafficking steps in which both docking and fusion have been intensively studied, and where probably most of the main players are known, is the fusion of early endosomes. Early endosomes form the first sorting station on which many routes of endocytosis converge (Maxfield and McGraw, 2004). They fuse not only with incoming endocytosed vesicles, but also with each other (referred to as homotypic fusion), which constitutes an important step in the recycling of material through the endosomal endomembrane system. Docking of early endosomes seems to be mainly regulated by the small GTPase Rab 5. Active (GTP-bound) Rab 5 is localized on the endosome membrane via its isoprenyl anchor. It recruits a complex of Rabaptin-5 and the Rab 5 guanine nucleotide exchange factor Rabex, which

This article was published online ahead of print in *MBC in Press* (http://www.molbiolcell.org/cgi/doi/10.1091/mbc.E08–05–0457) on October 8, 2008.

Address correspondence to: Reinhard Jahn (rjahn@gwdg.de).

together drive the exchange of GDP to GTP in Rab 5, resulting in a positive feedback loop that induces the further accumulation of the active GTPase on the membrane (Stenmark *et al.*, 1995; Lippe *et al.*, 2001). Active Rab 5 also recruits the phospatidyl inositol (PI)-3 kinase hVps34 (Christoforidis *et al.*, 1999b), which increases the local PI-3-phosphate concentration. Active Rab5 and PI(3)P then function as a "coincidence" signal for the recruitment of the long coiled-coil protein early endosomal autoantigen 1 (EEA1; Mu *et al.*, 1995; Patki *et al.*, 1997; Simonsen *et al.*, 1998). EEA1 is a tethering protein essential for docking (Christoforidis *et al.*, 1999a) that is thought to cross-link endosomes by the formation of homodimers (Callaghan *et al.*, 1999).

Although there appears to be consensus that SNAREs are not involved in the initial tethering contact between organelles destined to fuse, it is debated whether they contribute by transinteractions to the establishment of a stably docked state in preparation for fusion. For instance, several recent studies suggest a function for the SNARE syntaxin 1 in the docking of synaptic vesicles (Hammarlund *et al.*, 2007) and of dense core vesicles (Hammarlund *et al.*, 2008) in neurons of *Caenorhabditis elegans*. Similarly, docking of chromaffin granules significantly reduced in chromaffin cells in which syntaxin 1 was destroyed by botulinum neurotoxins (de Wit *et al.*, 2006). These findings disagree with earlier studies where syntaxin was perturbed without any measurable effects on docking (Broadie *et al.*, 1995; O'Connor *et al.*, 1997; Fujiwara *et al.*, 2006), but it is possible that such changes are only detectable if high-pressure freezing procedures are used for the electron microscopic analysis (Hammarlund *et al.*, 2007, 2008). In addition to exocytotic vesicles, several studies suggest that docking of yeast vacuoles (a compartment comparable to mammalian lysosomes; Wickner and Haas, 2000) depends at least partly on SNARE proteins (Ungermann *et al.*, 1998; Laage and Ungermann, 2001).

Here we analyzed the involvement of SNARE proteins in the docking of mammalian early endosomes. We generated a new fluorescence-based in vitro assay for measuring docking of endosomes. The assay differentiates between docked and fused organelles, thereby allowing for studying both processes in parallel. As expected, both fusion and docking are active, energy-consuming processes. Also, perturbing Rab and EEA1 function reduced both fusion and docking. However, inhibiting SNARE function selectively perturbed fusion, but not docking.

MATERIALS AND METHODS

Antibodies

The monoclonal anti-Synaptobrevin Cl 69.1 antibody (Edelmann *et al.*, 1995) and the polyclonal G96 anti-Synaptophysin antibody (Jahn *et al.*, 1985) were described previously. The rabbit anti EEA1 serum used for the functional studies was raised against CLRRILQRTPGRV (Takamori *et al.*, 2006). Antibodies used for Western blotting were monoclonals directed against Rab 5 (Cl 621.1; Fischer von Mollard *et al.*, 1994) and EEA1, which was purchased from BD Biosciences (San Jose, CA). F_{ab} fragments against Syntaxin 6, Syntaxin 13, Vti 1a, and Vamp 4 were a kind gift from Dr. D. Zwilling (University of California).

Recombinant Proteins

All constructs were described before: Syntaxin 6 (residues 169-234; Zwilling *et al.*, 2007), Syntaxin 13 (residues 1-250), Vti1a (residues 1-192), and mutant αSNAP L294A (Brandhorst *et al.*, 2006). Recombinant proteins were expressed as His_6- or glutathione *S*-transferase (GST)-tagged fusion proteins and purified by Ni_2-agarose or glutathione-Sepharose, respectively. The tags of all proteins were removed by thrombin cleavage. All proteins were further purified by ion-exchange chromatography. GDP-dissociation inhibitor (GDI) was a kind gift from Roger Goody (MPI for Molecular Physiology, Dortmund, Germany).

Cell Culture and Internalization of Marker

PC12 cells (clone 251; Heumann *et al.*, 1983) were grown to confluence on 15-cm-diameter culture dishes in DMEM (with 5% FCS, 10% horse serum, 4 mM glutamine, and 100 U/ml each of penicillin and streptomycin) at 37°C in 10% CO_2. Cells were harvested by washing once with room-temperature PBS (150 mM NaCl/200 mM Na_2HPO_4, pH 7.4), adding trypsin/EDTA (2 ml per plate; Lonza, Cologne, Germany). Cells were washed with internalization medium (OptiMEM; Invitrogen, Karlsruhe, Germany; supplemented with 10 mM glucose), prewarmed, and incubated for 5 min with marker (10-kDa dextran labeled with Alexa 488 or Alexa 594, respectively; Invitrogen), dissolved in internalization medium. The internalization was stopped by diluting the cells in 10 ml of ice-cold PBS with 5 mg/ml BSA, and the cells were washed three times with the solution. For the Atto 647N-labeled dextran, we coupled amino-dextran (Sigma, Munich, Germany) with the NHS-ester of the dye (Atto-tec, Siegen, Germany), by using a conventional protocol (modified from Invitrogen).

Preparation of Subcellular Fractions and Rat Brain Cytosol

PC12 cells were homogenized as described (Holroyd *et al.*, 1999) with slight modifications. Briefly, the cell pellet was resuspended 1:4 in homogenization buffer (250 mM sucrose/3 mM imidazole/HCl, pH 7.4) with protease inhibitors (0.2 mM PMSF, 1 μg/ml leupeptin, 1 μg/ml aprotinin, and 0.7 μg/ml pepstatin) and homogenized by 10 passages through a stainless-steel ball homogenizer with a clearance of 20 μm. The homogenates were centrifuged for 15 min at 1200 ×*g*, and the resulting postnuclear supernatants (PNSs) were divided into aliquots and snap-frozen in liquid N_2. PNS fractions labeled with Alexa 488 and Alexa 594 were used for the cell-free interaction assay. Rat brain cytosol was prepared from fraction S2 by centrifugation at 300,000 × *g* for 30 min (Huttner *et al.*, 1983).

Cell-Free Interaction Assay

Reaction mixtures (50 μl volume) contained, as final concentrations, 4 mg/ml PNS, 2 mg/ml cytosol, 11.25 mM HEPES, pH 7.0, 1.35 mM magnesium acetate, 0.18 mM DTT, 45 mM potassium acetate, as an ATP-regenerating system, 3.2 mM ATP, 26 mM creatine phosphate, and 0.132 mg creatine kinase (800 U/mg; Roche, Basel, Switzerland) or, as an ATP-depleting system, 5 μl hexokinase (1500 U/ml dissolved in 250 mM glucose; Roche). If not indicated otherwise, the reaction time was 45–60 min. The reaction solutions were directly added onto coverslips (18-mm diameter; Marienfeld GmbH, Lauda-Königshofen, Germany) in 12-well plates (into 1 ml of PBS) and centrifuged at 5900 × *g* in a Multifuge4 centrifuge (Heraeus Instruments, Hanau, Germany) for 45 min. Coverslips were analyzed by using a Zeiss Axiovert 200M fluorescence microscope (Jena, Germany) with a 1.4 NA 100× objective and appropriate filter sets (see Brandhorst *et al.*, 2006).

Clustering Assay

Endosomes from baby hamster kidney (BHK) 21 cells were used in the assay, because their larger size allowed for better imaging than for PC12 endosomes. Early endosomes were purified as described previously (Bethani *et al.*, 2007) and incubated in vitro as indicated above for the cell-free interaction assay. Endosome concentration was adjusted to 0.1–0.2 mg/ml. After 45 min, aliquots of the reactions were centrifuged onto glass coverslips as above. The coverslips were then imaged in presence of the styryl dye FM 2–10 (Invitrogen), at a concentration of 20 μM. The images (captured via a CCD camera with a 1317 × 1035 Kodak chip) were analyzed as follows: the total fluorescence of each image was normalized to an arbitrary value (same for all images, in all experiments), the images were divided in 13 bins of 100-pixel width, and the SD value was calculated for each of the 13 bins. The mean SD was then calculated and was used as an indicator of clusters in the images. For conditions containing mainly single endosomes, the fluorescence signal was evenly distributed within the images, and the SD was low. The clusters generated bright spots in small areas in the images, thus causing a strong increase in the SD measurement.

Membrane Binding of Proteins

Reaction mixtures identical to the once in the interaction assay were incubated with the additions described in the respective experiments. The membrane was then pelleted by ultracentrifugation for 20 min at 135,000 × g in a TLA 55 rotor (Beckman, Krefeld, Germany). For the GDI samples we wanted to analyze the conditions directly at the start of the reaction and therefore minimized the centrifugation time to 10 min at 500,000 × *g* in a TLA 120.2 rotor (Beckman). Pellets were dissolved and analyzed by Western blotting. The signal was determined by densiometry as described (Bethani *et al.*, 2007),

normalized to the synaptobrevin signal, and then expressed as percent of the signal from the control reaction. Controls were incubated either 60 min for GTPγS and wortmannin or 10 min for GDI.

STED Microscopy

Samples were imaged using a TCS STED (Stimulated Emission Depletion) superresolution fluorescence microscope from Leica Microsystems GmbH (Mannheim, Germany), with a 1.4 NA 100× objective (Leica). Excitation was performed with a 635 nm diode laser, and depletion was achieved via a Spectra-Physics MaiTai tunable laser at 750 nm. Signal was detected by use of an Avalanche Photodiode. The system resolution limit is approximately 70–90 nm, measured by analysis of crimson-fluorescent beads (20 nm diameter, Invitrogen).

Data Analysis

Imaging was performed as previously described (Brandhorst *et al.*, 2006; Rizzoli *et al.*, 2006; Bethani *et al.*, 2007). Images performed in the red and green channel were then analyzed automatically by use of a self-written routine in Matlab (The Mathworks, Natick, MA). The images were first high-pass filtered, to remove noise, then thresholds of 4–6 pixels above background were applied, and all objects above the thresholds (excluding single pixels) were used further in the analysis. The intensity centers of the objects were determined, corrected for the shift between the images by use of multicolor fluorescent beads (identified from images taken in the blue channel, where only the beads were seen), and all distances from green centers of intensity to red centers of intensity were determined. The distance to the closest red neighbor was then obtained for each green object and used further in the analysis. Endosomes whose red and green intensity centers were within 112.5 nm from each other were considered to be fused (see Figure 1D). The 25-nm distance from 112.5 to 137.5 nm was not analyzed because these organelles could not be unambiguously assigned to either fusion or docking. Endosomes whose red and green intensity centers were within 137.5–512.5 nm from each other were counted as docked. The value obtained for docking was then corrected for endosome density on the coverslip by subtracting a baseline due to random positioning of the endosomes on the coverglass (the average percentage for the distances from 512.5 to 1012.50 nm).

RESULTS

A New Microscopy-based Assay for Early Endosomal Docking

We developed a new assay that is based on labeling active early endosomes during endocytosis. We labeled the organelles by fluid-phase uptake of either Alexa 488– or Alexa 594–conjugated dextran (see *Materials and Methods* for details), which, under our pulse-labeling conditions (5-min incubation at 37°C) specifically labels early endosomes (Gruenberg and Howell, 1987; Gruenberg *et al.*, 1989; Brandhorst *et al.*, 2006). PNSs were then isolated from the cells and used in in vitro reactions, which contained rat brain cytosol and an ATP-regenerating system, i.e., conditions under which endosome fusion is known to occur (Brandhorst *et al.*, 2006). Aliquots from the reactions were either spun down immediately onto coverslips (Figure 1A) or after 60 min of incubation (Figure 1B). The coverslips were then imaged by conventional epifluorescence microscopy. We have shown previously that organelles labeled by this method colocalize to a high extent with bona fide early endosomal markers, such as transferrin and the early endosomal, but not the ER-to-Golgi, SNAREs (Brandhorst *et al.*, 2006). Many yellow (colocalized) spots were observed after incubation, compared with virtually none in the control.

To characterize the size distribution of our endosomes in more detail, we used stimulated emission depletion (STED) microscopy, in which a "doughnut"-shaped depletion beam is applied to quench the surrounding of the excitation center (Willig *et al.*, 2006). As a consequence emitted light is only collected from the center of the excited spot, which leads to a substantial increase in resolution (~70 nm in our hands). To be able to use STED microscopy, we coupled dextran to a STED-suitable fluorescent Atto dye, and used it for fluid-phase uptake as above. The size distribution is unimodal and centers around 200 nm, with an average size of 227 ± 17 nm (>3000 endosomes were measured, from six independent experiments; see Supplemental Figure S1).

To differentiate docking from fusion, we determined the centers of intensity for all spots both in the red and green channel and then measured the distances to the closest spot of the opposite color. To calibrate the assay, we performed two imaging experiments with fluorescent beads of a size similar to endosomes (~200 nm in diameter, Figure 1, D and E; see also Supplemental Figure S1). First, we used multilabeled TetraSpeck beads (Invitrogen), to simulate fused endosomes and analyzed them as above. The histogram shows a single peak ($r = \sim 80$ nm). Theoretical considerations reveal that this is to be expected if 1) the localization along the two orthogonal axes are following a Gaussian distribution, with the maximum at $r = 0$, and 2) the normal distributions along both axes are independent of each other (Rayleigh distribution, see *Appendix*). Although assumption 1 is probably only an approximation, we checked assumption 2 by testing whether the direction of the vector r is random in a given field of beads. This was indeed the case (data not shown). Second, we used a mixture of beads that were either green or red (also ~200 nm in diameter), and we repeated the same imaging and analysis procedure. These beads show a broad distance distribution, with no overlap with the colocalization peak (Figure 1E).

Figure 1C shows a typical histogram (average of nine experiments) for an endosome (PNS) preparation incubated for 60 min at 37°C. The distance distribution shows two peaks. The first exhibits a maximum ~75 nm and thus precisely corresponds to the peak of the multicolored bead control, documenting that this peak represents vesicle populations in which the two dyes are colocalized. The second peak spans between ~150–500 nm, thus revealing a population of endosomes that are not fused but closely associated with each other. We conclude that the first peak of the endosome distance distribution (Figure 1C) represents fused endosomes (in agreement with previous investigations on the subject, (Brandhorst *et al.*, 2006; Rizzoli *et al.*, 2006; Bethani *et al.*, 2007), whereas the second peak represents docked endosomes, thus allowing for differentiating docking from fusion.

An alternative method for monitoring in vitro docking of organelles was previously described for yeast vacuoles. According to this procedure, clusters of organelles are differentiated from single organelles simply by addition of a fluorescent membrane probe (e.g., a styryl dye) at the end of the docking reaction, which allows for visualizing all membranes in the reaction mixture (Mayer and Wickner, 1997; Wang *et al.*, 2002). However, when we monitored clustering of gradient-purified endosomes with this procedure, no good correlation between fusion and docking was observable (Supplemental Figure S2). Importantly, clustering was completely independent of ATP, raising doubts whether clustering as observed by this assay reports specific docking of endosomes (see *Materials and Methods* for details).

Basic Requirements of Endosome Docking

We first tested whether energy is required for docking. Removing ATP from the reaction mixture or incubating on ice inhibits fusion, as previously described (Gruenberg *et al.*, 1989; Brandhorst *et al.*, 2006) and also brings the docking value close to background. Very similar results were obtained when the endosome reaction mixtures were prepared separately and only mixed immediately before centrifugation onto coverslips (Figure 2A).

To quantitate docking and fusion, we measured the fraction of endosomes that were fused (their green and red intensity centers within ~100 nm from each other) or docked (their

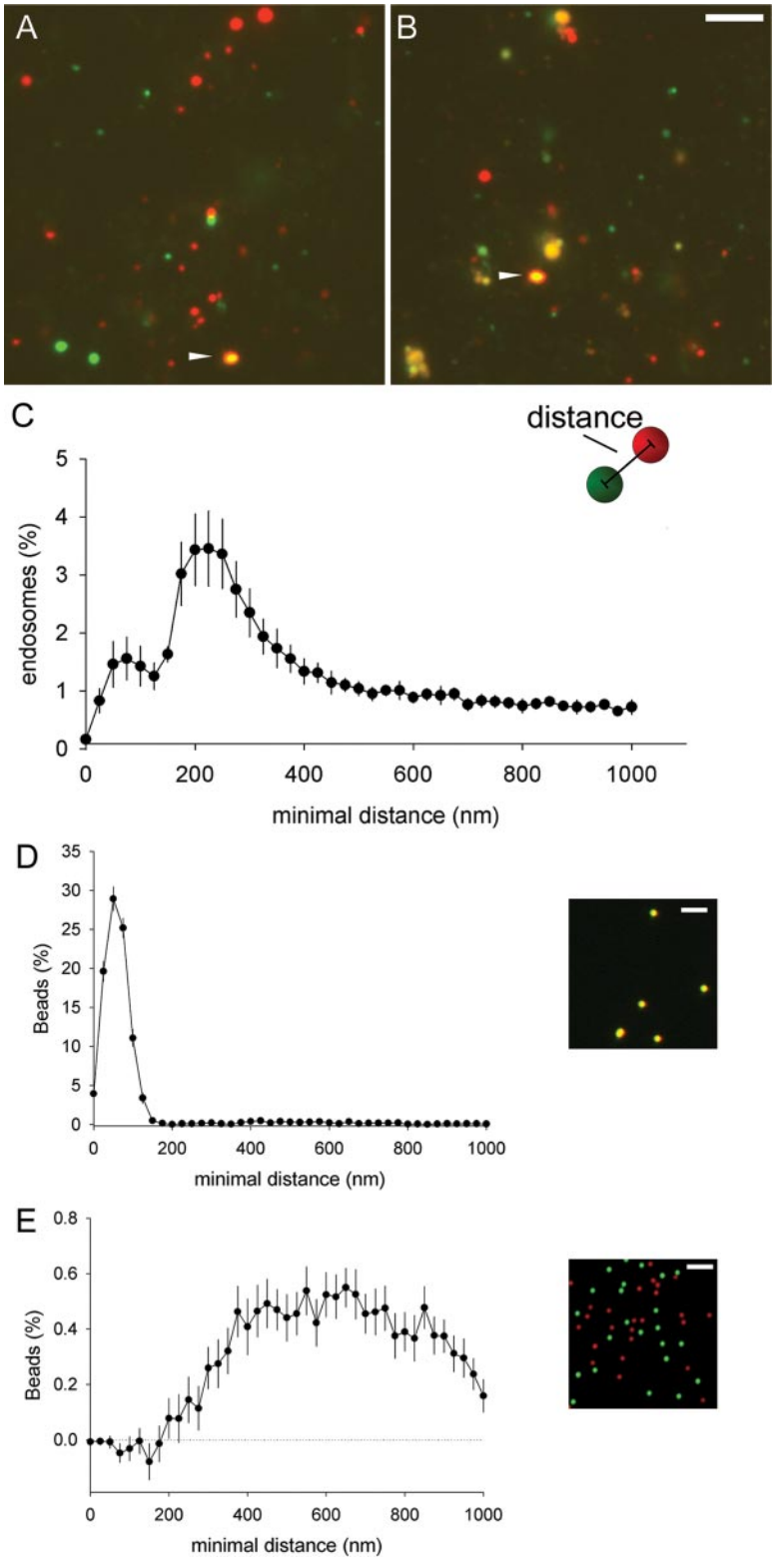

Figure 1. Establishing an early endosomal docking assay. Early endosomes were labeled by fluid-phase uptake of either Alexa 488- or Alexa 594-dextran and PNSs were prepared. The supernatants were combined in in vitro reactions containing rat brain cytosol, buffer, and an ATP-regeneration system and were spun down immediately onto coverslips as a negative control (A) or after 60 min of incubation at 37°C (B). The images acquired in the red and green channels were aligned using multicolor fluorescent beads (arrows) as reference. Scale bar, 5 μm. (C) The distance from each green endosome to its nearest neighbor in the red image was determined automatically using a MatLab routine (see *Materials and Methods*) and plotted as a histogram. Note the two peaks of the distribution. (D) TetraSpeck multicolor beads, 200 nm, used as a model for fused vesicles, were imaged and analyzed as in C. (E) Similarly sized single-color beads, used as a model for organelles that can get close together, but cannot fuse, were analyzed as above. The histograms in C and D were corrected for random colocalization (random overlap of the green and red spots) by subtracting the colocalization obtained between the green images and the mirror images of the red frames. Data are presented as mean ± SEM from nine independent experiments for the endosomes and three for the fluorescent beads.

intensity centers within ~150–500 nm from each other). The docking value was also corrected for accidental colocalization of endosomes as described in *Materials and Methods.* About 6% of the endosomes were fused in our reactions, which, as expected, was reduced to background values (~1%) upon ATP removal or incubation on ice (Figure 2B). Under conditions permissive for fusion, 15–20% of the endosomes were docked (but not fused). In contrast; no docking was observed in the absence of ATP and at low temperature (Figure 2C).

It has previously been shown that similar to yeast vacuoles (Peters and Mayer, 1998), fusion of early endosomes is dependent on the local release of Ca^{2+} ions because it is

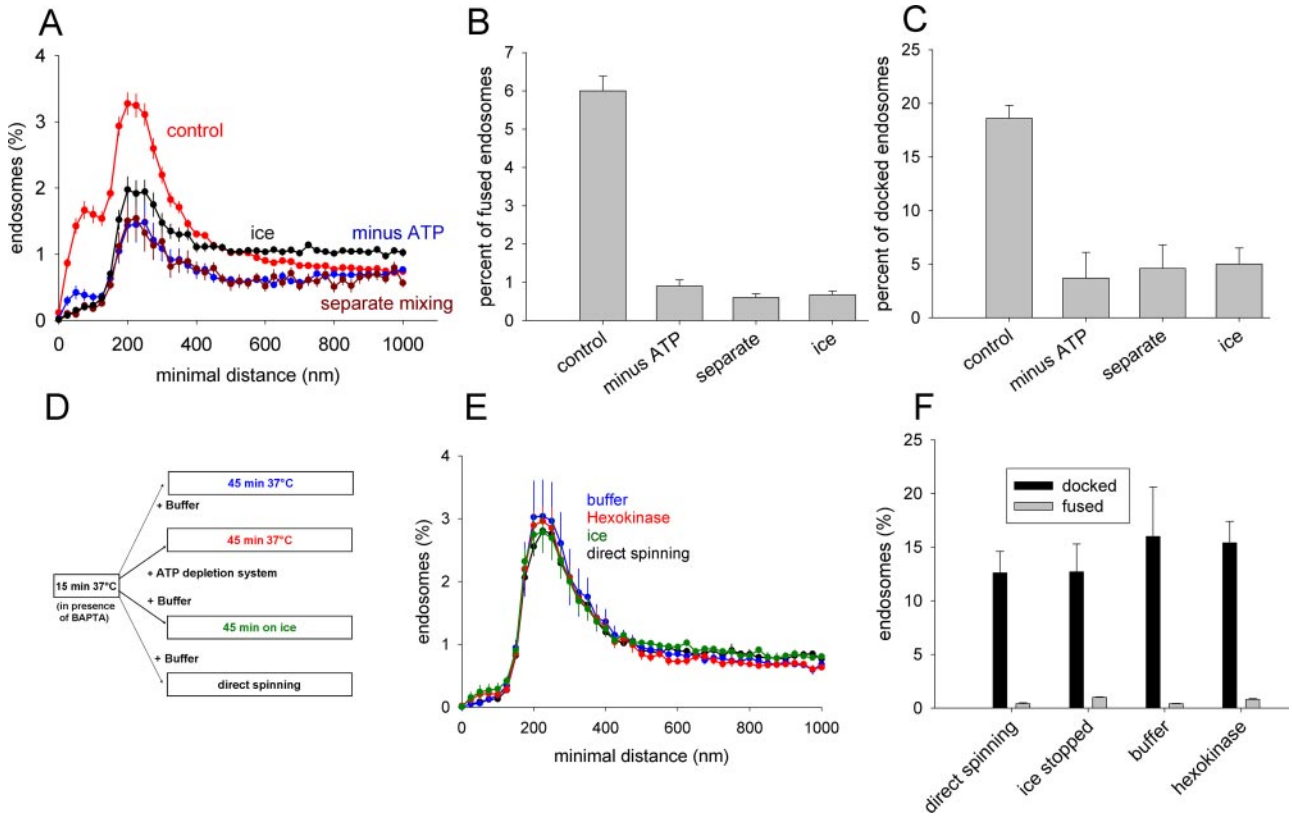

Figure 2. Basic requirements of the docking reaction. (A) In vitro reactions were performed in the presence or absence of ATP, either at 37°C or on ice. As a negative control, to check for the docking taking place during centrifugation of the organelles onto the coverslips, we incubated the red- and green-labeled PNS mixtures independently and combined them immediately before centrifugation (separate mixing). Note the substantial reduction of both peaks with lack of ATP or incubation on ice. (B and C) The fusion and docking values, essentially the percentages of endosomes corresponding to the first and second peak, respectively. Bars show the means from at least 13 independent experiments; error bars, ± SEM. (D) Scheme of the reaction performed to investigate the ATP dependence of the docking reaction. Mixtures containing cytosol, but no additional ATP, were incubated for 15 min in the presence of BAPTA, to allow for docking but not for fusion (see text, and Figure 4A, for effects of BAPTA). The reaction was then either 1) spun down directly, 2) stopped on ice, or 3) continued after addition of buffer or 4) an ATP-depletion system was added, to check whether docking is reversed in absence of ATP. (E) Nearest neighbor histograms of the controls and the ATP-depleted reaction appear similar. (F) Analysis of histograms presented in E. Bars show means from five to nine independent experiments; error bars, ± SEM.

inhibited by the fast Ca^{2+}-chelator BAPTA but not by the slower chelator EGTA (Holroyd *et al.*, 1999), suggesting that in the presence of BAPTA the system is arrested at a docked state. As shown in Figure 4A, this is indeed the case: In the presence of BAPTA the pool of fused endosomes is virtually abolished, whereas the pool of docked vesicles is largely unaffected. As expected, the slower calcium chelator EGTA, which is known not to affect fusion in this system (Holroyd *et al.*, 1999; Rizzoli *et al.*, 2006) had no significant effect on docking (three independent experiments, data not shown).

Being able to prevent docked endosomes to progress to fusion allowed for investigating whether not only initiation but also maintenance of docking is dependent on ATP. We tested this by incubating the endosomes for 15 min in the presence of BAPTA. The reaction was then either 1) spun down immediately, 2) stopped by placing the tubes on ice, or 3) continued after addition of buffer, or 4) an ATP-depletion system (hexokinase solution) was added, and the reaction continued for 45 min (Figure 2D). As shown in Figure 2, E and F, the amount of docking obtained in the first 15 min in presence of ATP persisted even after 45 min of ATP depletion, indicating that ATP is only needed for initiating docking but not for its maintenance.

Next we analyzed how dilution of the endosomes affects the docking reaction. Interestingly, docking turned out to be rather insensitive to dilution up to 100×, whereas fusion was substantially reduced (Figure 3, A–C). This suggests that, although reducing the probability for endosomes to meet in the reaction tube inhibits their fusion ability, their docking ability still persists. This is in line with the hypothesis that endosomes need to meet relatively early after the start of incubation in order to proceed to fusion (Barbieri *et al.*, 1998). We tested this by preincubating our endosomes separately for 10 min at 37°C in the reaction mixture before we combined them what yielded in a highly significant reduction of fusion but not docking (Figure 3, D–F). Apparently, the docking process is much more robust than fusion, with endosomes that meet late after the start of incubation being able to dock, but not to fuse.

Endosome Docking Is Independent of SNARE Function

The results described above document that with the novel assay described here it is possible to differentiate docking from fusion, thus allowing to investigate whether treatments known to block fusion also affect docking. In the next experiments, we have taken advantage of this assay to investigate

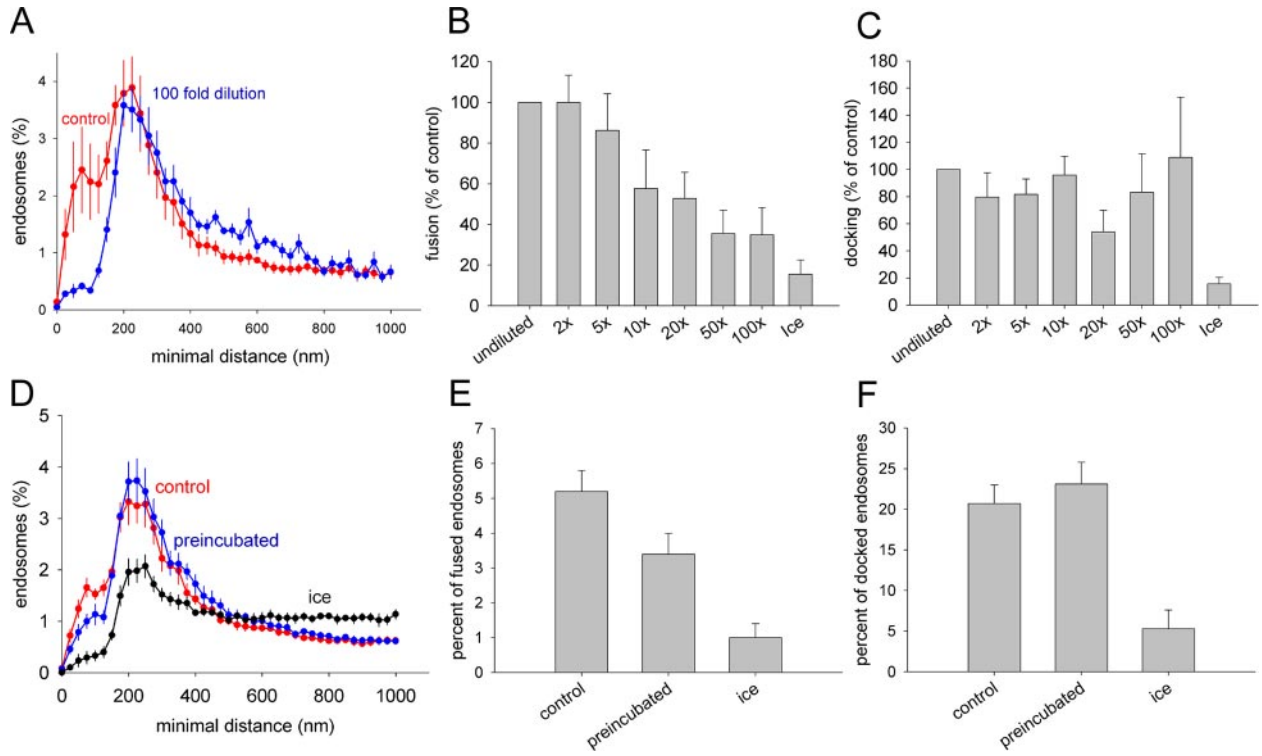

Figure 3. Differential sensitivity of docking and fusion to dilution and preincubation. (A–C) Endosomes were diluted up to 100-fold in the reaction mixture, incubated, and then analyzed by microscopy as above. Note the disappearance of the fusion (first) peak, but the persistence of the docking (second) peak. Fusion is significantly reduced by dilution ($p < 0.01$), whereas docking is relatively insensitive in the range analyzed. Bars (and curves in A) show means from five independent experiments; error bars, ± SEM. (D–F) Endosomes were preincubated separately for 10 min at 37°C and then combined for a further 45 min. Fusion is significantly reduced by this treatment ($p < 0.001$), whereas docking remains stable. Shown are averages from six independent experiments ± SEM.

the role of SNAREs in docking, an issue that is controversially discussed (see *Introduction*). Three complementary approaches were used.

First, we inhibited NSF by the addition of a mutant form of αSNAP (α-SNAP, which is unable to support ATP hydrolysis of NSF and thus functions as a dominant inhibitor of SNARE disassembly (Barnard *et al.*, 1997). Addition of αSNAP L294A (50 μM) strongly decreased fusion, but reduced docking only very mildly (Figure 4B), similar to the BAPTA effect.

Second, we added soluble fragments of the recently described early endosomal SNARE complex (Brandhorst *et al.*, 2006; Zwilling *et al.*, 2007), as competitive inhibitors. These proteins compete with the SNAREs on the early endosomal membrane for assembly and therefore reduce the amount of SNARE complex formation between the membranes destined to fuse (*trans*-complexes). We have shown previously that homotypic fusion of early endosomes is profoundly inhibited if a combination of the three Q-SNAREs syntaxin 13, syntaxin 6, and vti1a, is used. However, as shown in Figure 4C, docking remained basically unaltered although fusion was strongly reduced.

Finally, we added to the reaction a mixture of F_{ab} fragments directed against all of the early endosomal SNAREs (2 μg of each). We have shown previously that SNARE-specific F_{ab} fragments selectively block the function of SNAREs, thus providing convenient tools for interfering with specific SNAREs in in vitro reactions (Antonin *et al.*, 2000). Again, only a very small effect (compare with Supplemental Figure S3) on docking was observed although fusion was drastically inhibited (Figure 4D).

In conclusion, transinteraction between SNAREs is mandatory for fusion, but is not required for the docking of early endosomes.

Molecular Characteristics of Endosome Docking

To gain further insight into the molecular mechanisms underlying docking of early endosomes, we addressed several proteins that are known to function in endosome recycling. First, the actin cytoskeleton does not seem to be involved in the docking process, because perturbing actin via latrunculin A (Coue *et al.*, 1987) or phalloidin (Cooper, 1987) had no significant effects (Figure 5, A and B).

As already described in the *Introduction*, the EEA1 is thought to function as a major tethering factor that connects endosomes before fusion (Christoforidis *et al.*, 1999a). EEA1 is a Rab5 effector that also needs to bind to PI3-phosphate via its FYVE domain for effective recruitment to the endosomal membrane. To interfere with EEA1-binding, we used the PI-3 kinase inhibitor wortmannin (50 nM), which resulted in a decrease of EEA1 membrane association by ~70% (Figure 5C). Under these conditions, docking was strongly inhibited (~60%). Fusion was also reduced but to a somewhat lower degree (Figure 5, A and B). Furthermore, incubation of endosomes with an EEA1 antiserum or with a FYVE peptide that competes with EEA1-binding to PI(3)P (McBride *et al.*, 1999) reduced docking but had no major effects on fusion (see *Discussion*). The effect of the EEA1 antiserum was fully neutralized by applying the peptide against the antibody was raised (see Figure 5, A and B). Together, these data confirm that EEA1 function is instrumental for effective and/or stable docking.

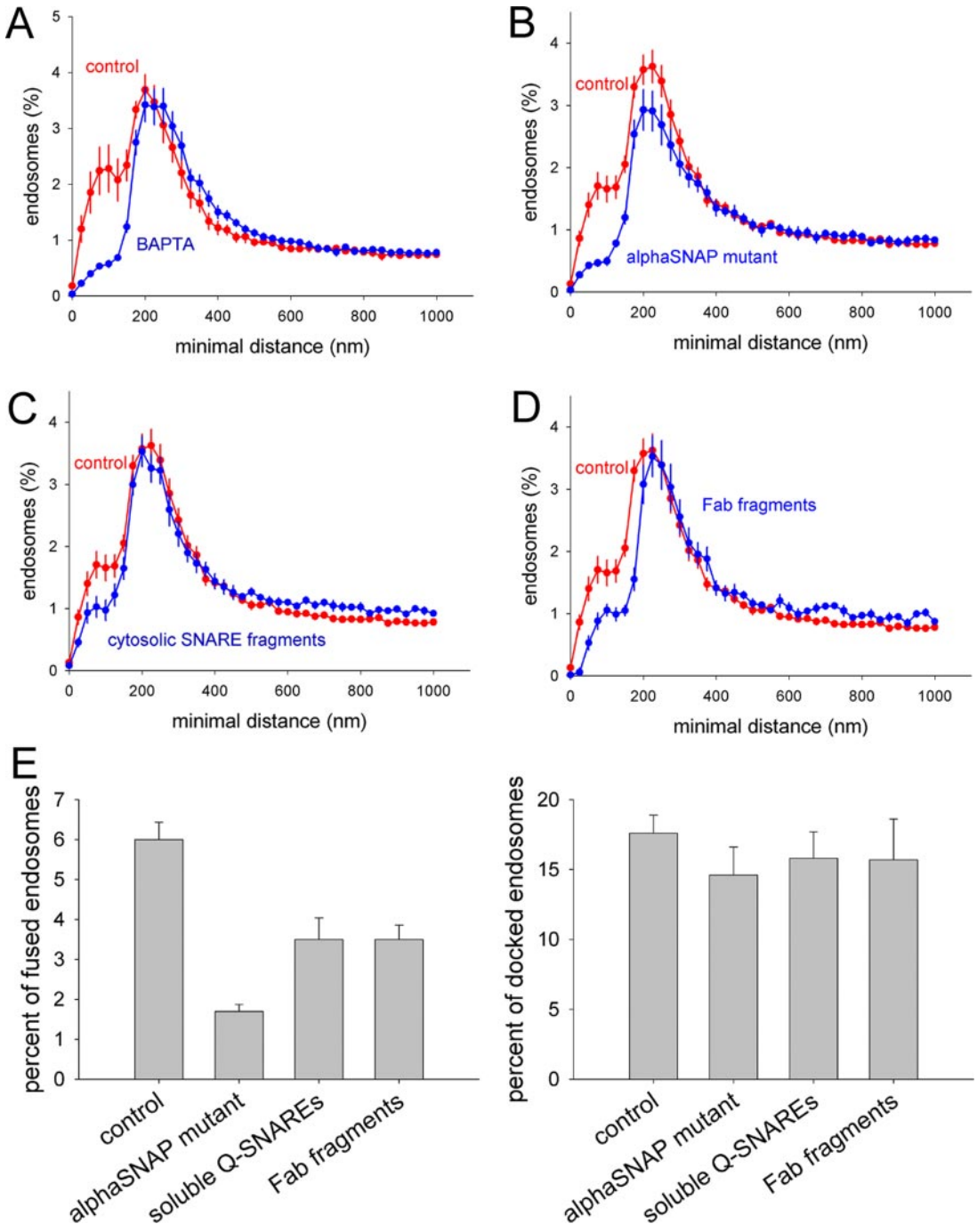

Figure 4. Early endosomal SNAREs do not act as docking factors. (A) In vitro reactions were performed in presence of 10 mM BAPTA, to inhibit fusion, but not docking. (B–D) The reactions were performed in presence of inhibitors of SNARE function: 50 μM of αSNAP L294A (B), cytosolic fragments of Sx6, Sx13, and Vti1a (30 μM each, C), or F_{ab} fragments anti-Vamp 4, Vti1a, Sx6, and Sx13 (2 μg of each, D). (E) Analysis of the histograms in A–D shows that fusion is strongly reduced by all of these reagents, whereas docking is barely affected. Bars, means from at least six independent experiments ± SEM.

We next investigated the role of Rab GTPases on docking. In the fusion of early endosomes, Rab5 has been shown to orchestrate the assembly of docking complexes and to function upstream of EEA1. We added GTPγS to the reactions to increase the fraction of the active, GTP-bound conformation of Rab proteins. Surprisingly, we observed that docking was reduced rather than potentiated. This finding was explained by the fact that GTPγS caused a loss of EEA1 from the membranes (Figure 5C), although the fraction of membrane-bound Rab 5 did increase. Finally, the combination of wortmannin with GTPγS reduced docking even further. Thus, although GTPγS increased the amount of active Rab 5, it nevertheless reduced the membrane-bound fraction of EEA1. This suggests that binding of EEA1 to Rab 5 may not be sufficient for its recruitment to the membrane in absence of other

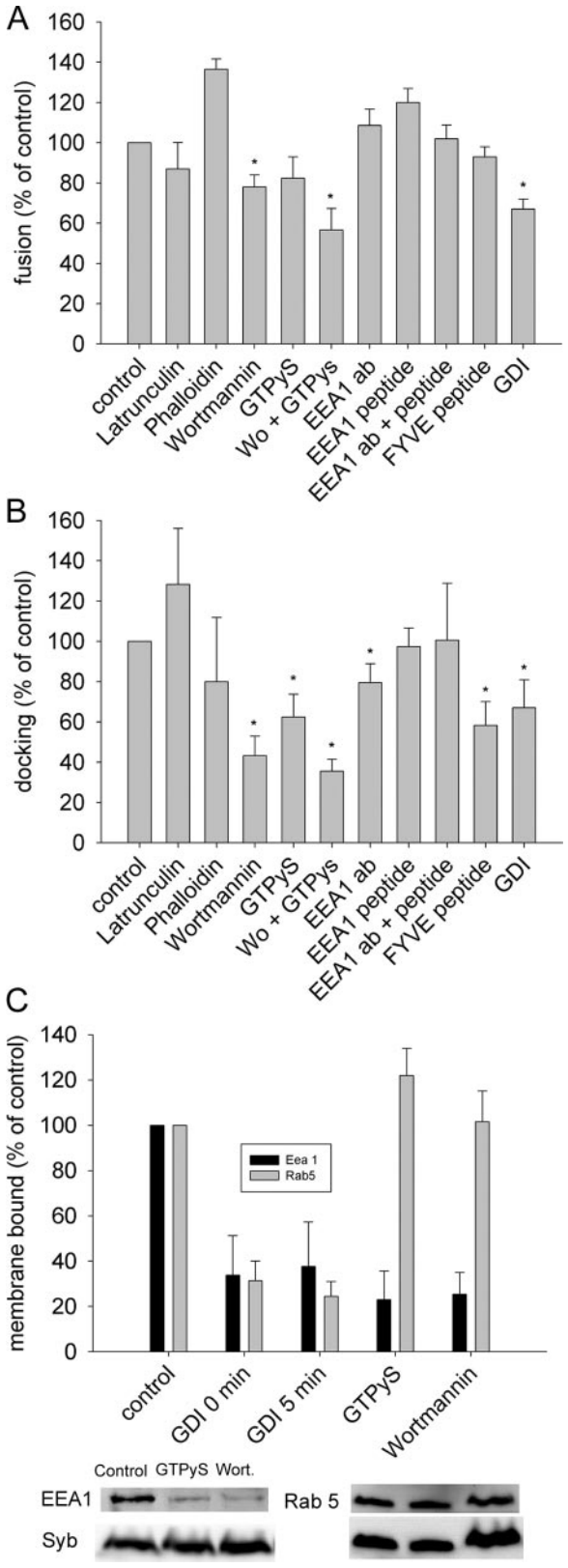

Figure 5. EEA1 is involved in the docking process. A number of putative docking factors were tested for their influence on fusion (A) and docking (B). The concentrations used were 15 μM for latrunculin A, 10 μM for phalloidin, 50 nM for wortmannin, 200 μM for GTPγS, 10 μM for GDI, 600 μM for the FYVE peptide, and ~60 μl/ml for the anti-EEA1 serum. GDI and the anti-EEA1 serum were incubated for 30 min on ice, before the reaction, to allow Rab 5 release and antibody binding, respectively. Bars show means from three to 11 independent experiments ± SEM. Significant inhibition (relative to control) is indicated ($p < 0.05$, Student's t test). (C) Membrane localization of Rab 5 and EEA1 was analyzed by using the same reaction mixtures and protocols as in the imaging experiments, i.e., with 30-min preincubation on ice for GDI. After 60 min at 37°C (or 0 and 5 min for GDI) the reactions were ultracentrifuged and the amounts of Rab5 or EEA1 found in the pellets were analyzed. Bars show means from three to four independent experiments; error bars, ± SEM.

interactions (Jones *et al.*, 1998; Simonsen *et al.*, 1998; Lawe *et al.*, 2002). Why membrane levels of EEA1 are reduced in the GTPγS-treated reactions remains obscure, with one possible explanation being that the PI-3-kinase (hVps34) needs to be activated by a process involving a GTPase cycle that would be blocked by GTPγS.

The presence of Rab proteins on the membrane is, however, necessary for docking. This became evident when we treated our PNS with 10 μM GDI, which binds to Rab proteins in the GDP-bound (inactive) form and dissociates them from the membrane. Samples were preincubated for 30 min on ice in the presence of GDI and were then either centrifuged directly or incubated for 5 min at 37°C. At the start of the reaction, i.e., after preincubation with GDI, the membrane-bound fraction of Rab 5 is already reduced by over 60% compared with the control. Under these conditions, docking was significantly inhibited. The loss of Rab 5 from the membrane was accompanied by a comparable loss of EEA1, in line with the view that Rab5 mediates docking via its effector EEA1 (Raiborg *et al.*, 2001).

DISCUSSION

In the present study we describe a novel fluorescence-based in vitro assay that reliably differentiates between docking and fusion of early endosomes. Our data show that docking is a time- and ATP-dependent process. SNARE function is not needed for docking. Conversely, we show that EEA1 association with the endosome membrane is instrumental for docking, confirming the role of EEA1 as tethering/docking factor.

As our assay depends on endocytotic labeling of endosomes, it only reports docking of functionally defined, bona fide early endosomes. With this approach, we avoided a significant problem associated with organelle clustering assays, where the identity of the organelles is difficult to determine (i.e., in such assays the organelles visualized may all be endosomes, but not necessarily recently endocytosed, or active, endosomes). Indeed, organelle clustering was clearly not energy-dependent, unlike fusion or bona fide docking. This finding correlates well with results from other in vitro systems, where clustering only shows an ATP dependence when the assay conditions are substantially changed from those of a normal fusion reaction (e.g., through a strong reduction of the salt concentration, Mayer and Wickner, 1997).

Interestingly, our data also show that fusion and docking do not correlate perfectly. Although only ~6% of the endosomes have fused after 60 min, about three times more remain in the docked state (see Figures 2–4 and Supplemental Figure S3) and are apparently unable to proceed further to fusion, as fusion has already largely ceased at this point (data not shown and Brandhorst *et al.*, 2006). In addition, some factors like wortmannin and the FYVE peptide inhib-

ited docking much strongly than fusion (see Figure 5, A and B), indicating that not all endosomes that are able to dock are equally able to fuse. Conversely, fusion was reduced by dilution, but docking was not (see Figure 3, A–C).

The dilution results indicate that in these conditions the endosomes were able to meet and dock, but were no longer able to proceed to fusion. This correlates well with the observation that early endosomes are less fusogenic after separate preincubation at 37°C (Barbieri *et al.,* 1998 and unpublished observations), which suggests that the endosomes are primed for fusion at the start of incubation, and then must meet and fuse within a limited amount of time. Dilution (or separate incubation; see Figure 3, D–F) prolongs this period, and results in nonfusogenic endosomes, a hypothesis first put forward in the yeast vacuole system (Mayer and Wickner, 1997; Xu *et al.,* 1997). This also provides a relatively simple explanation for the substantial amount of docked, but not fused endosomes: they would be organelles that met too late in the reaction and were beyond the point of fusion.

The specificity of the docking process is underlined by the fact that although the labeled endosomes constitute only a very small fraction of all organelles (data not shown), a substantial percentage (20–25%) still manage to find each other, even when they are strongly diluted (Figure 3). This is all the more remarkable when one considers that our assay only measures the amount of green endosomes interacting with red ones, while ignoring the interactions between endosomes labeled with the same dye. Including these interactions would bring the fraction of endosomes fusing or docking to each other to 60–75%. Furthermore, we only measure one round of docking/fusion in our assay (an endosome fusing or docking onto a green-red pair would not be accounted for), and thus even this estimate is likely lower than the total fraction of active organelles.

These observations are in line with the current understanding of docking/tethering (Sztul and Lupashin, 2006; Cai *et al.,* 2007) as a process mediated by an interplay of small GTPases like Rabs and long tethering molecules or mulitsubunit complexes. Indeed, the results from our assay suggest that fusion, but not docking, required SNARE function. Interestingly, our findings differ somewhat from those in one in vitro system where fusion has been thoroughly investigated, the yeast vacuole (Wickner, 2002). Although the differences between the systems may explain the different results (with the yeast vacuole corresponding to the late endosome/lysosome of the mammalian cell, and not to the early endosome), it is also likely that a number of experimental details contribute to the different interpretations.

In vitro docking of yeast vacuoles was suggested to depend on transinteractions between SNARE proteins mainly because 1) transinteraction between SNAREs was observed when fusion was inhibited by late stage (i.e., post docking) inhibitors such as microcystin-LR (Ungermann *et al.,* 1998), 2) vacuole clustering depends on ATP/NSF activity (Mayer and Wickner, 1997), and 3) one may be able to disengage putative *trans*-SNARE complexes by excess NSF without influencing fusion (Ungermann *et al.,* 1998, 1999; Peters *et al.,* 2001). However, as suggested above, some of these results may depend strongly on the experimental conditions. When a new fusion assay was used, microcystin-LR did not seem to inhibit vacuole fusion, but rather the activation/activity of alkaline phosphatase (ALP), which was used as a marker for vacuolar fusion in the original assays (Mayer and Wickner, 1997; Jun and Wickner, 2007). Also, in one report vacuole clustering was shown to be SNARE independent (Wang *et al.,* 2003), and vacuole clustering also seems to be independent of ATP under buffer conditions used for the fusion reaction (Jun and Wickner, 2007). Finally, it is still debated whether the NSF-sensitive SNARE complexes monitored in the work mentioned were bona fide *trans*-complexes or rather *cis*-complexes formed in the (previously) fused organelles.

Although our data show that endosome docking is not affected by interference with SNARE function, we do not believe that there is no functional cross-talk between the molecular machinery involved in docking and SNARE proteins. Several lines of evidence indicate that docking proteins directly bind to SNAREs. For instance, EEA1 has been shown to interact both with syntaxin 6 (Mills *et al.,* 2001) and syntaxin 13 (McBride *et al.,* 1999), i.e., two of the SNAREs involved in the fusion of early endosomes (Brandhorst *et al.,* 2006). It is conceivable that such binding plays a role in regulating the transition from tethering to fusion (Sztul and Lupashin, 2006). Furthermore, we cannot exclude that SNAREs are involved in stabilizing and maintaining a docked state. This may be particularly relevant in cases where progress from docking toward fusion does not occur constitutively (as is the case for endosome fusion) but is regulated, resulting in prolonged and reversible docked states (as in synapses: Hammarlund *et al.,* 2007, 2008) or in certain neuroendocrine cells).

APPENDIX

Rayleigh Distribution of Distances between Centers of Intensity

Let's assume that the measurements for the positional distance (distance difference between the red and the green channel) of a multicolored bead along one axis follow a Gaussian distribution, with the mean being at $x = 0$ and $y = 0$, respectively. This assumption is only an approximation but appears reasonable for distance values below the point spread function of the microscope. The distribution P_x is described by the standard formula for a normal distribution (SD: σ):

$$P_x(x) = \frac{1}{\sigma\sqrt{2\pi}} e^{-x^2/2\sigma^2}$$

and similar for $P_y(y)$.

We assume (as experimentally confirmed) that P_x and P_y are uncorrelated. In this case, the probability distribution of the distance $r = \sqrt{x^2 + y^2}$ is described by a Rayleigh distribution

$$P(r) = \frac{r}{\sigma^2} e^{-r^2/2\sigma^2}$$

It follows that although the probability density function exhibits a maximum for both independent distributions at $x = 0$ and $y = 0$, respectively, the probability density function for $r = 0$ ($x = 0$,$y = 0$) is $P(r) = 0$. The maximum of the

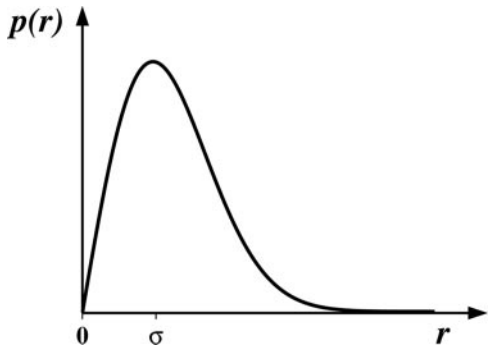

function P(r) is identical with the SD σ (the value where the first derivative = 0):

ACKNOWLEDGMENTS

The authors are indebted to R. Goody for providing purified GDP-dissociation inhibitor, to A. Jahn (University of Edinburgh) and H. Grubmüller (MPI for Biophysical Chemistry) for help with the mathematics and D. Zwilling (San Francisco) for F_{ab} fragments. We thank C. Schäfer for technical assistance. U.G. is supported by a fellowship from the Deutsche Forschungsgemeinschaft Research Training Grant 521. S.V.B. acknowledges the support of the MSc/PhD program 'Molecular Biology' (International Max Plank Research School;). S.O.R. has been the recipient of a postdoctoral fellowship from the Human Science Frontier Program. S.O.R. acknowledges the support of a grant from the German Ministry of Research and Education (BMBF; Nanolive, Vesikelbewegungen durch Nanoauflösung).

REFERENCES

Antonin, W., Holroyd, C., Tikkanen, R., Honing, S., and Jahn, R. (2000). The R-SNARE endobrevin/VAMP-8 mediates homotypic fusion of early endosomes and late endosomes. Mol. Biol. Cell *11*, 3289–3298.

Barbieri, M. A., Hoffenberg, S., Roberts, R., Mukhopadhyay, A., Pomrehn, A., Dickey, B. F., and Stahl, P. D. (1998). Evidence for a symmetrical requirement for Rab5-GTP in in vitro endosome-endosome fusion. J. Biol. Chem. *273*, 25850–25855.

Barnard, R. J., Morgan, A., and Burgoyne, R. D. (1997). Stimulation of NSF ATPase activity by alpha-SNAP is required for SNARE complex disassembly and exocytosis. J. Cell Biol. *139*, 875–883.

Bethani, I., Lang, T., Geumann, U., Sieber, J. J., Jahn, R., and Rizzoli, S. O. (2007). The specificity of SNARE pairing in biological membranes is mediated by both proof-reading and spatial segregation. EMBO J. *26*, 3981–3992.

Brandhorst, D., Zwilling, D., Rizzoli, S. O., Lippert, U., Lang, T., and Jahn, R. (2006). Homotypic fusion of early endosomes: SNAREs do not determine fusion specificity. Proc. Natl. Acad. Sci. USA *103*, 2701–2706.

Broadie, K., Prokop, A., Bellen, H. J., O'Kane, C. J., Schulze, K. L., and Sweeney, S. T. (1995). Syntaxin and synaptobrevin function downstream of vesicle docking in *Drosophila.* Neuron *15*, 663–673.

Cai, H., Reinisch, K., and Ferro-Novick, S. (2007). Coats, tethers, Rabs, and SNAREs work together to mediate the intracellular destination of a transport vesicle. Dev. Cell *12*, 671–682.

Callaghan, J., Simonsen, A., Gaullier, J. M., Toh, B. H., and Stenmark, H. (1999). The endosome fusion regulator early-endosomal autoantigen 1 (EEA1) is a dimer. Biochem. J. *338*(Pt 2), 539–543.

Christoforidis, S., McBride, H. M., Burgoyne, R. D., and Zerial, M. (1999a). The Rab5 effector EEA1 is a core component of endosome docking. Nature *397*, 621–625.

Christoforidis, S., Miaczynska, M., Ashman, K., Wilm, M., Zhao, L., Yip, S. C., Waterfield, M. D., Backer, J. M., and Zerial, M. (1999b). Phosphatidylinositol-3-OH kinases are Rab5 effectors. Nat. Cell Biol. *1*, 249–252.

Cooper, J. A. (1987). Effects of cytochalasin and phalloidin on actin. J. Cell Biol. *105*, 1473–1478.

Coue, M., Brenner, S. L., Spector, I., and Korn, E. D. (1987). Inhibition of actin polymerization by latrunculin A. FEBS Lett. *213*, 316–318.

de Wit, H., Cornelisse, L. N., Toonen, R. F., and Verhage, M. (2006). Docking of secretory vesicles is syntaxin dependent. PLoS ONE *1*, e126.

Edelmann, L., Hanson, P. I., Chapman, E. R., and Jahn, R. (1995). Synaptobrevin binding to synaptophysin: a potential mechanism for controlling the exocytotic fusion machine. EMBO J. *14*, 224–231.

Fischer von Mollard, G., Stahl, B., Walch-Solimena, C., Takei, K., Daniels, L., Khoklatchev, A., De Camilli, P., Sudhof, T. C., and Jahn, R. (1994). Localization of Rab5 to synaptic vesicles identifies endosomal intermediate in synaptic vesicle recycling pathway. Eur. J. Cell Biol. *65*, 319–326.

Fujiwara, T., Mishima, T., Kofuji, T., Chiba, T., Tanaka, K., Yamamoto, A., and Akagawa, K. (2006). Analysis of knock-out mice to determine the role of HPC-1/syntaxin 1A in expressing synaptic plasticity. J. Neurosci. *26*, 5767–5776.

Gruenberg, J., Griffiths, G., and Howell, K. E. (1989). Characterization of the early endosome and putative endocytic carrier vesicles in vivo and with an assay of vesicle fusion in vitro. J. Cell Biol. *108*, 1301–1316.

Gruenberg, J., and Howell, K. E. (1987). An internalized transmembrane protein resides in a fusion-competent endosome for less than 5 minutes. Proc. Natl. Acad. Sci. USA *84*, 5758–5762.

Hammarlund, M., Palfreyman, M. T., Watanabe, S., Olsen, S., and Jorgensen, E. M. (2007). Open syntaxin docks synaptic vesicles. PLoS Biol. *5*, e198.

Hammarlund, M., Watanabe, S., Schuske, K., and Jorgensen, E. M. (2009). CAPS and syntaxin dock dense core vesicles to the plasma membrane in neurons. J. Cell Biol. *180*, 483–491.

Heumann, R., Kachel, V., and Thoenen, H. (1983). Relationship between NGF-mediated volume increase and "priming effect" in fast and slow reacting clones of PC12 pheochromocytoma cells. Role of cAMP. Exp. Cell Res. *145*, 179–190.

Holroyd, C., Kistner, U., Annaert, W., and Jahn, R. (1999). Fusion of endosomes involved in synaptic vesicle recycling. Mol. Biol. Cell *10*, 3035–3044.

Huttner, W. B., Schiebler, W., Greengard, P., and De Camilli, P. (1983). Synapsin I (protein I), a nerve terminal-specific phosphoprotein. III. Its association with synaptic vesicles studied in a highly purified synaptic vesicle preparation. J. Cell Biol. *96*, 1374–1388.

Jahn, R., and Scheller, R. H. (2006). SNAREs—engines for membrane fusion. Nat. Rev. Mol. Cell. Biol. *7*, 631–643.

Jahn, R., Schiebler, W., Ouimet, C., and Greengard, P. (1985). A 38,000-dalton membrane protein (p38) present in synaptic vesicles. Proc. Natl. Acad. Sci. USA *82*, 4137–4141.

Jones, A. T., Mills, I. G., Scheidig, A. J., Alexandrov, K., and Clague, M. J. (1998). Inhibition of endosome fusion by wortmannin persists in the presence of activated Rab5. Mol. Biol. Cell *9*, 323–332.

Jun, Y., and Wickner, W. (2007). Assays of vacuole fusion resolve the stages of docking, lipid mixing, and content mixing. Proc. Natl. Acad. Sci. USA *104*, 13010–13015.

Kawasaki, F., Mattiuz, A. M., and Ordway, R. W. (1998). Synaptic physiology and ultrastructure in comatose mutants define an in vivo role for NSF in neurotransmitter release. J. Neurosci. *18*, 10241–10249.

Klenchin, V. A., and Martin, T. F. (2000). Priming in exocytosis: attaining fusion-competence after vesicle docking. Biochimie *82*, 399–407.

Laage, R., and Ungermann, C. (2001). The N-terminal domain of the t-SNARE Vam3p coordinates priming and docking in yeast vacuole fusion. Mol. Biol. Cell *12*, 3375–3385.

Lawe, D. C., Chawla, A., Merithew, E., Dumas, J., Carrington, W., Fogarty, K., Lifshitz, L., Tuft, R., Lambright, D., and Corvera, S. (2002). Sequential roles for phosphatidylinositol 3-phosphate and Rab5 in tethering and fusion of early endosomes via their interaction with EEA1. J. Biol. Chem. *277*, 8611–8617.

Lippe, R., Miaczynska, M., Rybin, V., Runge, A., and Zerial, M. (2001). Functional synergy between Rab5 effector Rabaptin-5 and exchange factor Rabex-5 when physically associated in a complex. Mol. Biol. Cell *12*, 2219–2228.

Maxfield, F. R., and McGraw, T. E. (2004). Endocytic recycling. Nat. Rev. Mol. Cell Biol. *5*, 121–132.

Mayer, A., and Wickner, W. (1997). Docking of yeast vacuoles is catalyzed by the Ras-like GTPase Ypt7p after symmetric priming by Sec18p (NSF). J. Cell Biol. *136*, 307–317.

McBride, H. M., Rybin, V., Murphy, C., Giner, A., Teasdale, R., and Zerial, M. (1999). Oligomeric complexes link Rab5 effectors with NSF and drive membrane fusion via interactions between EEA1 and syntaxin 13. Cell *98*, 377–386.

Mills, I. G., Urbe, S., and Clague, M. J. (2001). Relationships between EEA1 binding partners and their role in endosome fusion. J. Cell Sci. *114*, 1959–1965.

Mu, F. T., Callaghan, J. M., Steele-Mortimer, O., Stenmark, H., Parton, R. G., Campbell, P. L., McCluskey, J., Yeo, J. P., Tock, E. P., and Toh, B. H. (1995). EEA1, an early endosome-associated protein. EEA1 is a conserved alpha-helical peripheral membrane protein flanked by cysteine "fingers" and contains a calmodulin-binding IQ motif. J. Biol. Chem. *270*, 13503–13511.

O'Connor, V. *et al.* (1997). Disruption of syntaxin-mediated protein interactions blocks neurotransmitter secretion. Proc. Natl. Acad. Sci. USA *94*, 12186–12191.

Patki, V., Virbasius, J., Lane, W. S., Toh, B. H., Shpetner, H. S., and Corvera, S. (1997). Identification of an early endosomal protein regulated by phosphatidylinositol 3-kinase. Proc. Natl. Acad. Sci. USA *94*, 7326–7330.

Peters, C., Bayer, M. J., Buhler, S., Andersen, J. S., Mann, M., and Mayer, A. (2001). Trans-complex formation by proteolipid channels in the terminal phase of membrane fusion. Nature *409*, 581–588.

Peters, C., and Mayer, A. (1998). Ca^{2+}/calmodulin signals the completion of docking and triggers a late step of vacuole fusion. Nature *396*, 575–580.

Raiborg, C., Bremnes, B., Mehlum, A., Gillooly, D. J., D'Arrigo, A., Stang, E., and Stenmark, H. (2001). FYVE and coiled-coil domains determine the specific localisation of Hrs to early endosomes. J. Cell Sci. *114*, 2255–2263.

Rizzoli, S. O., Bethani, I., Zwilling, D., Wenzel, D., Siddiqui, T. J., Brandhorst, D., and Jahn, R. (2006). Evidence for early endosome-like fusion of recently endocytosed synaptic vesicles. Traffic *7*, 1163–1176.

Schikorski, T., and Stevens, C. F. (2001). Morphological correlates of functionally defined synaptic vesicle populations. Nat. Neurosci. *4*, 391–395.

Simonsen, A., Lippe, R., Christoforidis, S., Gaullier, J. M., Brech, A., Callaghan, J., Toh, B. H., Murphy, C., Zerial, M., and Stenmark, H. (1998). EEA1 links PI(3)K function to Rab5 regulation of endosome fusion. Nature *394*, 494–498.

Stenmark, H., Vitale, G., Ullrich, O., and Zerial, M. (1995). Rabaptin-5 is a direct effector of the small GTPase Rab5 in endocytic membrane fusion. Cell *83*, 423–432.

Sztul, E., and Lupashin, V. (2006). Role of tethering factors in secretory membrane traffic. Am J. Physiol. Cell Physiol. *290*, C11–C26.

Takamori, S. *et al*. (2006). Molecular anatomy of a trafficking organelle. Cell *127*, 831–846.

Ungermann, C., Sato, K., and Wickner, W. (1998). Defining the functions of trans-SNARE pairs. Nature *396*, 543–548.

Ungermann, C., Wickner, W., and Xu, Z. (1999). Vacuole acidification is required for trans-SNARE pairing, LMA1 release, and homotypic fusion. Proc. Natl. Acad. Sci. USA *96*, 11194–11199.

Wang, L., Merz, A. J., Collins, K. M., and Wickner, W. (2003). Hierarchy of protein assembly at the vertex ring domain for yeast vacuole docking and fusion. J. Cell Biol. *160*, 365–374.

Wang, L., Seeley, E. S., Wickner, W., and Merz, A. J. (2002). Vacuole fusion at a ring of vertex docking sites leaves membrane fragments within the organelle. Cell *108*, 357–369.

Waters, M. G., and Hughson, F. M. (2000). Membrane tethering and fusion in the secretory and endocytic pathways. Traffic *1*, 588–597.

Wickner, W. (2002). Yeast vacuoles and membrane fusion pathways. EMBO J. *21*, 1241–1247.

Wickner, W., and Haas, A. (2000). Yeast homotypic vacuole fusion: a window on organelle trafficking mechanisms. Annu. Rev. Biochem. *69*, 247–275.

Willig, K. I., Rizzoli, S. O., Westphal, V., Jahn, R., and Hell, S. W. (2006). STED microscopy reveals that synaptotagmin remains clustered after synaptic vesicle exocytosis. Nature *440*, 935–939.

Xu, Z., Mayer, A., Muller, E., and Wickner, W. (1997). A heterodimer of thioredoxin and I(B)2 cooperates with Sec18p (NSF) to promote yeast vacuole inheritance. J. Cell Biol. *136*, 299–306.

Zwilling, D., Cypionka, A., Pohl, W. H., Fasshauer, D., Walla, P. J., Wahl, M. C., and Jahn, R. (2007). Early endosomal SNAREs form a structurally conserved SNARE complex and fuse liposomes with multiple topologies. EMBO J. *26*, 9–18.